TRIBOLOGICAL BEHAVIORS OF Cu-BASED COMPOSITES WITH $NbSe_2$ AND TiB_2

J. F. LI[a], B. CHEN[a*], H. TANG[a], S. ZHANG[a], C. LI[a,b*]
[a]*School of Materials Science and Engineering, Jiangsu University, Key Laboratory of Tribology of Jiangsu Province, Zhenjiang, 212013, P. R. China*
[b]*School of Mechanical Engineering, Jiangsu University, 301, Xuefu Road, Zhenjiang, 212013, Jiangsu Province, P. R. China*

The tribological properties of Cu-based composites with niobium diselenide ($NbSe_2$) and titanium diboride (TiB_2) were investigated systematically by a ball-on-disk multi-functional tribometer, scanning electron microscopy equipped with EDS and Laser Raman Spectrometer. Results showed that the friction-reducing and anti-wear properties of copper matrix composites were enhanced greatly, especially for the simultaneous addition of 10%wt.$NbSe_2$ and 10%wt.TiB_2, which was attributed to the synergetic effect of $NbSe_2$ and TiB_2.

(Received September 17, 2017; Accepted December 9, 2017)

Keyword: Cu-based composites, Friction-reducing, Synergetic effect

1. Introduction

At present, copper and silver alloys are the most widely used throughout the world[1-9]. Especially, Cu-based composites with good electrical and thermal properties, easy processing, and low cost have always attracted considerable interests. However, its applications were limited due to its low strength and hardness. Therefore, intensive studies have been carried out to enhance mechanical and tribological properties of by the addition of fillers. It is indicated that Cu/Al_2O_3 composite has high strength, good conductivity and thermal conductivity, but also good arc erosion resistance and abrasion resistance[10]. S.C.Tjong et al [11] have found that Cu/SiC composites improve the abrasive wear resistance of pure copper significantly under the applied loads of 15–55 N. Shukla et al [12] observed that the presence of stable Cr_2Nb precipitates in Cu-based composites results in excellent retention of mechanical and electrical properties.

Recently, attention is paid to transition metal dichalcogenides $NbSe_2$, because it is hexagonal layered structure, and possess tribological properties as good as graphite or MoS_2. Zheng et al found [13] that the addition of $NbSe_2$ could effectively reduce the plastic deformation of the substrate, making the frction and wear properties of composite has greatly improved. Tang et al [14] reported that the copper matrix composites containing appropriate $NbSe_2$ nanofiber contents had low electrical resistivity and excellent anti-friction and wear properties.

In this work, $NbSe_2$ and TiB_2 were synthesized via a facile thermal solid-state reaction and self-propagating high temperature reaction, respectively. Cu-based composites with $NbSe_2$ and TiB_2 as the solid self-lubricant and strengthening phase were prepared using powder metallurgy (P/M) method[15-17]. Their synergetic effect on the tribological properties of composites were

*Corresponding authors: chenbb@ujs.edu.cn

investigated systematically. Besides, the corresponding enhancement mechanisms were discussed in detail.

2. Experimental

2.1. Materials

$NbSe_2$ were successfully fabricated via a facile thermal solid-state reaction and the details of the fabrication process were given elsewhere[18]. TiB_2 were synthesized by self-propagating high temperature synthesis reaction using B_2O_3, Ti and Mg powders. B_2O_3, Ti and Mg powders were well mixed at a molar ratio of 1:1:3 firstly. The balls with diameter of 8mm were made of hard alloy. The charge ratio (ball to powder mass ratio) employed was 10:1. The milling time and speed were set at 72h and 250 rpm, respectively. Then, the well-mixed powders were put into the graphite reactor, which were pumped into a vacuum state by vacuum pump. Argon was used as the synthetic atmosphere at the pressure of 0.1MPa. Finally, the whole experiment was carried out by lighting tungsten successfully. Subsequently, the quartz was gradually cooled to room temperature due to condensate water, opened, and the mixed powders with TiB_2 and MgO were obtained. The synthetic powders were soaked under mechanical agitation in hydrochloric acid solution of 2mol/L after mechanical crushing with the aim of removing MgO impurity phase. TiB_2 were obtained by vacuum suction and vacuum drying.

Six kinds of composites used in this study were made by powder metallurgy (P/M) technique and were denoted as CTN0, CTN1, CTN2, CTN3, CTN4 and CTN5 (The detailed components are shown in Table 1). The preparation process of Cu-based composites was summarized as follows [19]: copper powders, $NbSe_2$ and TiB_2 were mechanically mixed by high energy ball-milling in vacuum with the milling speed of 250 rpm for 12 h. Balls and vials were made of hard alloy. The charge ratio (ball to powder mass ratio) employed was 10:1. After being mixed and dried, the powders were initially compacted at cold state in a special designed die at the pressure of 500 Mpa for 10 min. Next, the powders were heated to 850°C and held for 2h in argon atmosphere. After the samples cooled to room temperature under protective atmosphere, as-prepared specimen were ground to remove the layers on the surfaces and polished mechanically with successive grades of emery papers down to 1200 grit, 5μm up to a mirror finish for the following tests and analyses.

2.2. Characterization

The phase compositions of $NbSe_2$,TiB_2 and Cu-based composites were identified by a D8 advance (Bruker-AXS) diffractometer with Cu Ka radiation (λ = 0.1546 nm). The morphology of $NbSe_2$ and TiB_2 were characterized by scanning electron microscopy (SEM, S-3400N) equipped with EDS. The morphology and phase compositions of wear scars of specimens was examined via Field Emission Scanning Electron Microscope (SEM, JSM-7001F) equipped with EDS and Laser Raman Spectrometer(DXR).

2.3 Physical properties

The density of as-prepared specimens was measured via using Archimedes's principle. The vickers hardness was determined by a vickers hardness Tester (MH-5) with a load of 500g and

a dwell time of 15s. The average of all the ten readings was taken as density and hardness of the samples in Table 1.

2.4 Tribological test

The tribological properties of Cu-based composites were appraised using a ball-on-disk multi-functional tribometer (UMT-2). The as-prepared materials were disk, and were cleaned with acetone and then dried in hot air before test. The counterpart was the stainless ball with diameter of 4mm produced from GCr15 steel. The drying sliding friction and wear tests were conducted under the load of 7N and a sliding velocity of 0.006m/s. The testing time was 30 min and the sliding radius was 3 mm. The friction coefficients were recorded automatically by an on-line data acquisition system attached to the tribometer. The profile of the worn surface was measured using a SURFCOM 130A roughmeter and the wear volume was determined as V=AL, where *A* was the cross section area of worn scar, *L* was the length of worn scar. The specific wear rate, W=V/SF, was determined as a function of the wear volume divides by the sliding distance S in meter and the applied load F in Newton. In addition, all tribological tests and measurements were carried out at least four times under the same condition and the average values are reported.

3. Results and discussion

3.1. Characterization

Fig.1 shows the SEM images and XRD patterns of TiB_2. It could be seen that as-prepared TiB_2 particles with diameters of about 2~3μm (Fig.1a). Fig.1b shows that all observed diffraction peaks could be systematically indexed to TiB_2 (JCPDS No.47–1639). No peaks from other phases were detected. Besides, EDS analyzed in Fig.1c shows the powder only consisted of element Ti and B, furthermore, the atom ratio between Ti and B were close to 1:2, which suggested that pure TiB_2 were obtained successfully. In addition, it could be seen that $NbSe_2$ had a hexagonal layered structure, which possessed the average diameter of 1.5μm and thickness of 200 nm (Fig.1d). EDS analyzed in Fig.1f indicates the atom ratio of Nb and Se elements were about 1:2. Besides, the XRD pattern of $NbSe_2$ is shown in Fig.1e, all labeled diffraction peaks of as-prepared $NbSe_2$ coincided with the values of standard card (PDF No.65-7464). It could be also clearly found that the intensity of (002) layered peak was stronger than any other peaks, which further suggested $NbSe_2$ possessed the laminar structure. No impurities produced during the sintering process, which showed that as-prepared $NbSe_2$ possessed high purity.

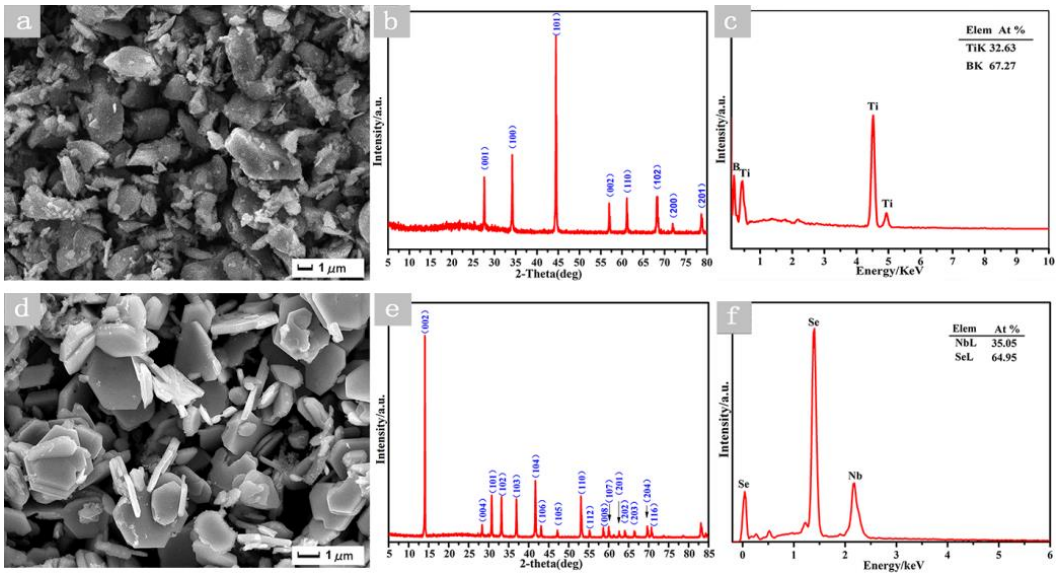

Fig.1 SEM image of TiB_2 and $NbSe_2$ microparticles (a),(d), XRD pattern of TiB_2 and $NbSe_2$ (b),(e) and EDS analysis of TiB_2 and $NbSe_2$ (c),(f)

3.2 Phase compositions, density, and hardness

The XRD patterns of Cu-based composites are exhibited in Fig.2. It could be clearly found that the diffraction peaks primarily matched well with Cu phase in all samples. However, as $NbSe_2$ content increased, Cu_xNbSe_2 as well as a small amount of Cu_2Se phases were formed and the diffraction peaks of $NbSe_2$ disappeared, which was due to a complex reaction between Cu and $NbSe_2$ at high temperature[20-22]. New compounds between Cu and TiB_2 was not found, because the high melting point ceramic TiB_2 was not soluble in solid copper during the sintering process.

As an example of specimen CTN3, the microstructure and elemental distribution are given in Fig.3. It could be seen that specimen possessed a dense and homogeneous microstructure, which indicated the well-distributed lubricating and strengthening phases had good interfacial bonding with copper particles. According to the EDS analysis, the red area was the continuous bulk Cu phase, the black phase and deep gray phase were TiB_2 and $Cu_xNbSe_2/NbSe_2$, respectively and their distribution were very uniform in the matrix. The presence of these phases was also confirmed by XRD pattern of CTN.

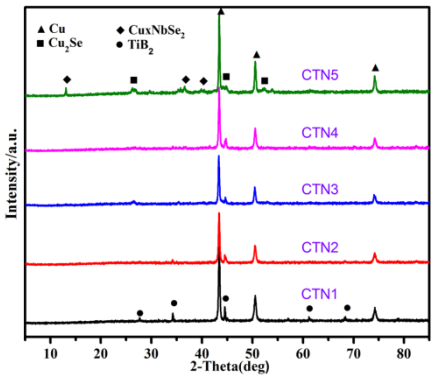

Fig.2 the XRD patterns of as-prepared Cu-based composites

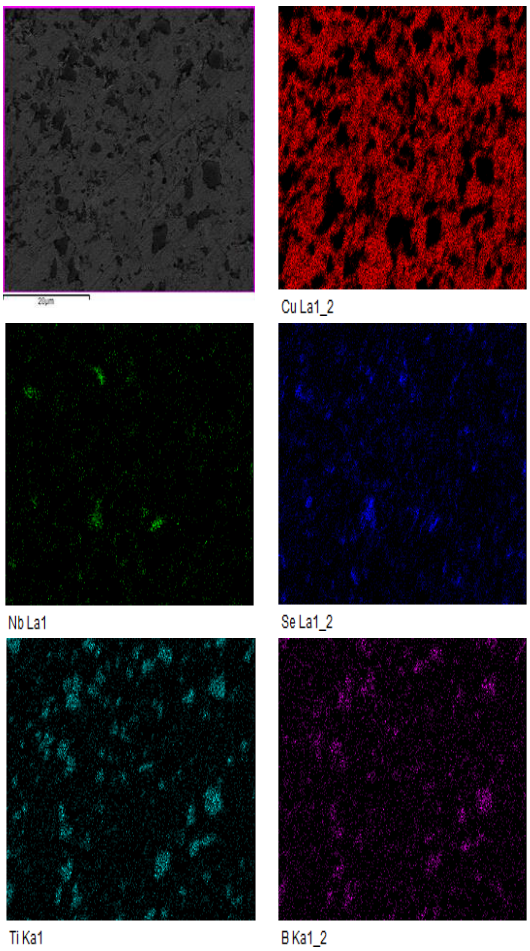

Fig. 3. Microstructure and elemental distribution of specimen CTN3

Table 1 The chemical compositions, density and hardness of Cu-based composites

Specimen	Cu	TiB_2	$NbSe_2$	Sintered density (g/cm^3)	Microhardness (HV)
CTN 0	100	0	0	6.47	80
CTN 1	80	20	0	6.53	138
CTN 2	80	15	5	6.79	116
CTN 3	80	10	10	6.87	108
CTN 4	80	5	15	6.97	103
CTN 5	80	0	20	7.13	93

Table 1 presents the density and hardness of Cu-based composites. It could be seen that the addition of TiB_2 and $NbSe_2$ could increased the density of Cu-based composites, which could be two reasons that one was the addition of TiB_2 and $NbSe_2$ could restricted the expand of composites[18].Another was compared with pure copper, much smaller particles size of TiB_2 and $NbSe_2$ led to the compactness of Cu-based composites increase during sintering process, which increased effectively the density of Cu-based composites. The reason is comfirmed by Fig.4. It

could be found that TiB_2 served as an enhanced phase to increase the hardness of Cu-based composites. With the addition of NbSe increased, the hardness of composites decreased obviously, which could be ascribed to the absence of fine and uniformly distributed TiB_2.

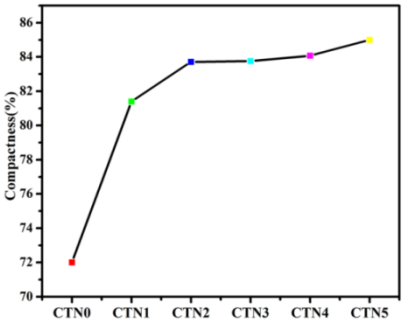

Fig.4 the variation of compactness of Cu-based composites

3.4 Friction and wear behaviors

Fig.5a shows the variations of friction coefficient of Cu-based composites at the condition of 7N-0.00612m/s under dry friction. It could be noted that the friction coefficient of CTN0 was the highest compared with that of other composites. The friction coefficient of CTN1, CTN2, and CTN3 had noticeable reduction with the increasing content of $NbSe_2$ and obtained the lowest value of approximately 0.14, which might be the existence of $NbSe_2$ and Cu_xNbSe_2 determined by their laminated structure in Cu-based composites [20-22]. However, as the content of $NbSe_2$ further exceeded, the coefficients of friction gradually tended to rise to high value from 0.14 to 0.22. This might be related to the agglomerates of the excessive $NbSe_2$[19]. Fig.5b exhibits the wear rate of Cu-based composites after wear tests. It could be seen that specimen CTN0 possessed the highest wear rate about $7.3\times10^{-3}mm^3.N^{-1}m^{-1}$. The wear rate of specimens decreased sharply from $7.5\times10^{-5}\,mm^3.N^{-1}m^{-1}$to $6.9\times10^{-5}\,mm^3.N^{-1}m^{-1}$, when the content of $NbSe_2$ increased to 5wt.%. With the $NbSe_2$ content continuously raised to 10wt.%, the wear rate of specimen CTN3 was the lowest among six samples and reached its minimum value about $2.1\times10^{-5}\,mm^3.N^{-1}m^{-1}$, which was about 300 times lower than that of specimen CTN0. Besides, with the content of $NbSe_2$ further increasing, the wear rate of composites increased due to the decreased TiB_2 content. TiB_2 particles could increase the hardness of composites, and further endowed the composites with good load-carrying capacity. Therefore, it could be concluded that appropriate content of $NbSe_2$ and TiB_2 could greatly improve the tribological properties of Cu-based composites.

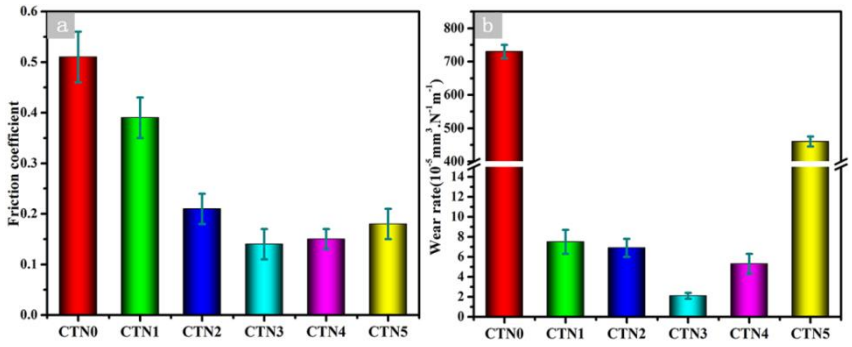

Fig.5 Friction coefficients and wear rate of Cu-based composites sliding against stainless steel ball under dry friction

Fig.6 illustrates noncontact three-dimension cross-section images of wear tracks obtained on surface of CTN1, CTN3 and CTN5 under the applied load of 7N. It could be clearly seen that the width of wear track reduced from 0.52 mm to 0.36 mm with the incorporation of 10wt.%$NbSe_2$. As the content of $NbSe_2$ continuously increased, the width of corresponding composite wear track became wide. This was consistent with the results shown in Fig.5b.

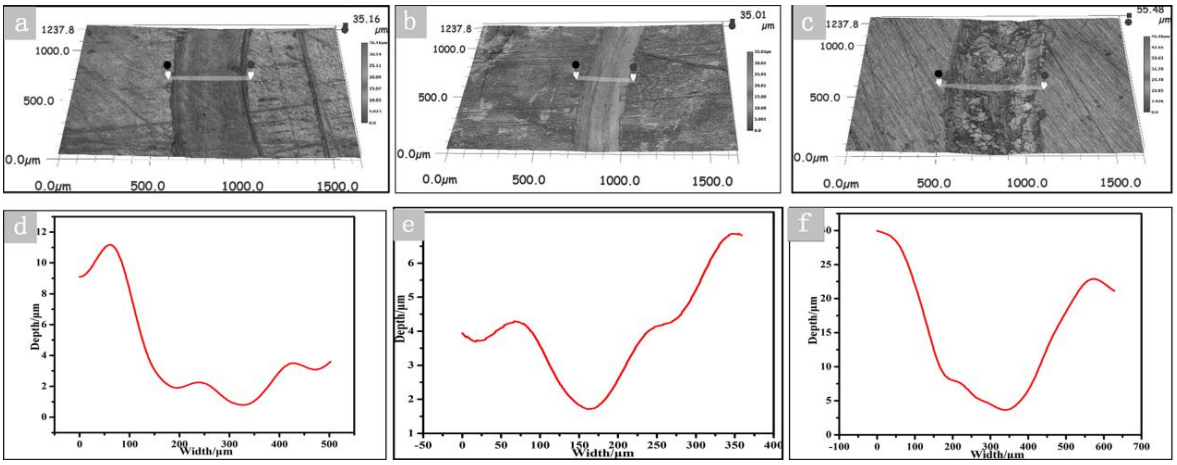

Fig.6 Noncontact three-dimension cross-section images of wear tracks obtained on surface of CTN1(a),CTN3(b) andCTN5(c) under the applied load of 7N;(d,e,f) Corresponding cross-section profiles of the wear tracks

3.5 Evaluation of worn surfaces

Fig.7a-d show the morphologies of worn surface of specimens at the condition of 7N-0.00612m/s after wear tests. In Fig.7a, micro-plough, furrows, and serious plastic delamination were observed on the worn surface, indicating that the wear mechanism was dominated by abrasive wear and plastic delamination, which was consistent with the result of pure copper possessing the highest wear rate. For CTN1 (Fig.7(b)), grooves, cracks, slight plough and plastic deformation could be found on the worn surface. It meant that the severe plastic deformation was largely restricted during the sliding process by the incorporation of TiB_2. C.S.Ramesh [23] reported that TiB_2 possessing high elastic modulus, hardness, and strength, could effectively increase the capacity for resisting plastic deformation. It was worth noting that the worn surface of CNT3 was dense and smooth, as shown in Fig.7(c). A continuous tribo-film covered on the surface could reduce the friction coefficient and wear rate in the process of friction in comparison with specimen CTN1 and CTN0. Furthermore, TiB_2 with the excellent mechanical properties existed homogeneously on the tribo-film could carry the load applied on the sliding surface, which enhanced obviously wear resistance of composites [22]. That was consistent with the result of specimen CTN3 with the lowest friction coefficient and wear rate. For CTN5, large number of cracks, debris, grooves and pits could be seen on the worn surface (Fig.7 (d)). The formed tribo-film of the worn surface of CTN5 was destroyed by the heavy load due to the absence of TiB_2 , which deteriorated seriously the wear resistance of specimen CTN5.

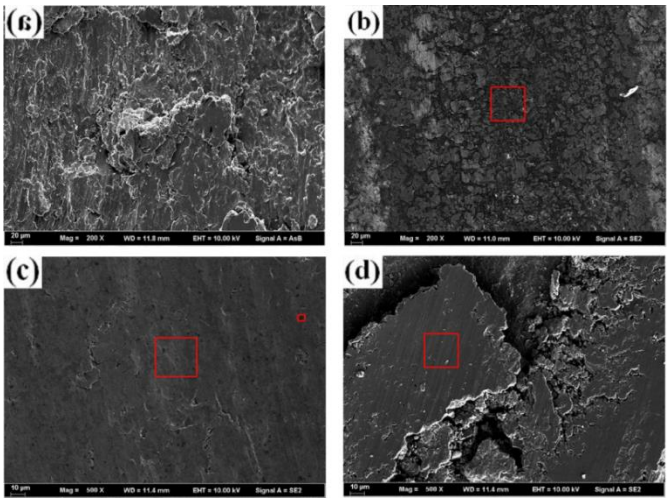

Fig. 7. SEM micrographs of the worn surface of specimen CTN0(a), CTN1(b), CTN3(c), CTN5(d)

In order to further determine the phase compositions of tribo-film. Specimen CTN3 with excellent tribological properties was chosen for further analysis. Raman spectrum of the worn surface of CTN3 composite before and after wear test are indicated in Fig.8. $NbSe_2$, Fe_2O_3 and CuO were detected in the tribo-film compared with unworn surface. The peak of $NbSe_2$ in the Cu-based composites became stronger after wear test, which demonstrated more $NbSe_2$ was reformed during the sliding process. This might be because high friction heat led to some Cu_xNbSe_2 decompose. Furthermore, it could be clearly seen that the position of the peak of $NbSe_2$ with noticeable angular widening of the relative profiles shifted negatively from 230 $cm^{-1}$to 215 cm^{-1}after wear test, which meant the in-plane structure of $NbSe_2$ was greatly broken. Overall, $NbSe_2$ sheets were exfoliated into thinner sheets during friction and wear process. Furthermore, Fig.9 gives the EDS of the red squares on the worn surfaces of CTN1, CTN3 and CTN5. EDS analyzed at the marked regions in Fig.9b indicated that Fe, Nb, Se, Ti and O elements were detected on the worn surface of specimen CTN3 except Cu element, which was consistent with Fig.9. It also could be seen that uniformly dispersed black particles adhered on the tribo-film. EDS analyzed at the marked black particles in Fig.9c suggested Ti and B elements were found on the tribo-film and the atom ratio was close to 1:2, which suggested uniformly dispersed black particles were TiB_2.

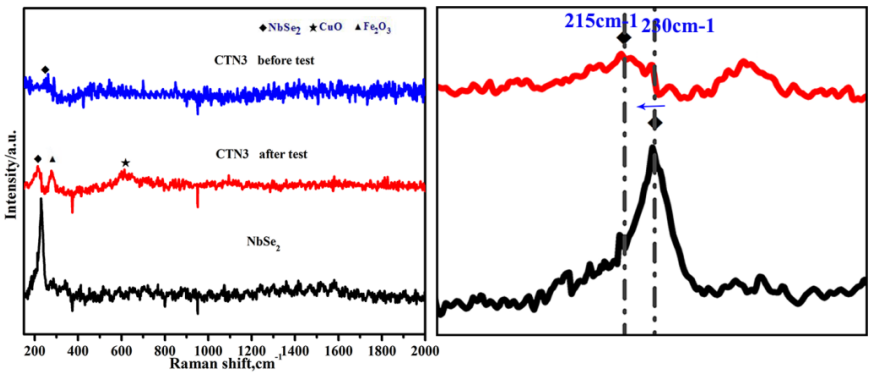

Fig.8 Raman spectrum of the glaze layer of the worn surface of sample CTN3 before and after wear test

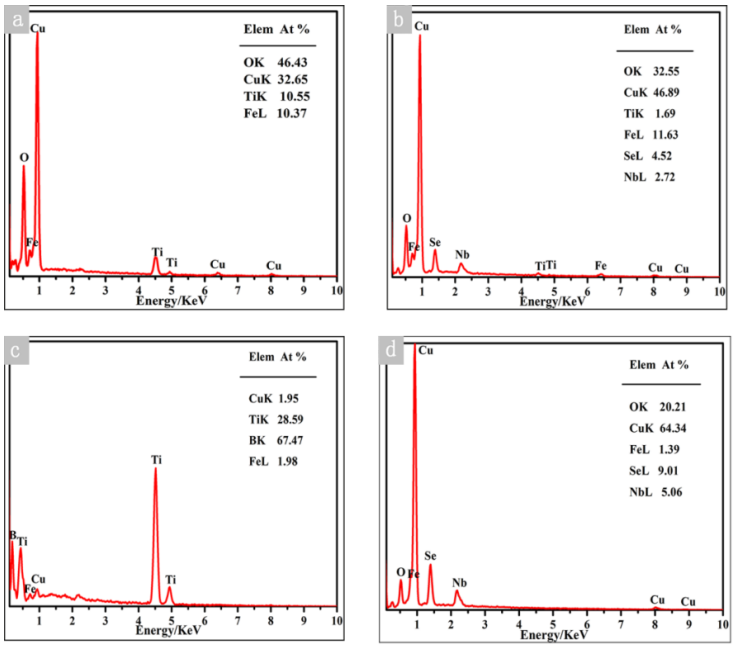

Fig.9 EDS analysis of the worn surface of Cu-based composites: (a)CTN1, (b)、(c)CTN3,(d)CTN5

Fig.10 shows a schematic of wear mechanisms of Cu-based composites during the friction and wear properties. This could be summarized that during the sliding process, Cu matrix was worn off, newly formed $Cu_xNbSe_2$and $NbSe_2$ were exposed on the worn surface. Some Cu_xNbSe_2 might be broken down into $NbSe_2$ and Cu due to high friction heat. Low amount of Cu and Fe came from the counterpart were oxidized into CuO and Fe_2O_3. Besides, some $NbSe_2$ sheets with low shear strength were sheared by the shear force. The tribo-film was mainly composed of Cu_xNbSe_2 and $NbSe_2$ to avoid the direct contact between Cu-based composites and counterpart under contact stresses, which had not only a significant anti-friction effect, but also a protective action for the worn surface[24]. TiB_2 existed homogeneously on the tribo-film, which could increase the carrying capacity of the tribo-film under dry friction conditions.

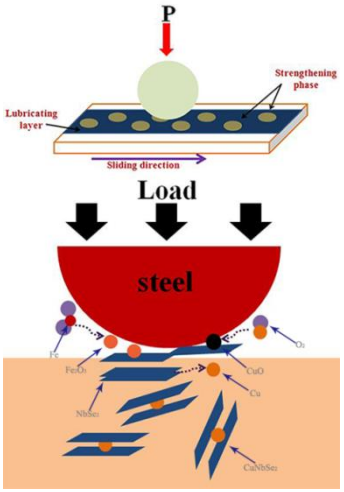

Fig.10 A schematic illustration that showed the wear mechanisms of Cu-based composites during the friction and wear properties

4. Conclusions

$NbSe_2$ and TiB_2 were successfully prepared by a facile thermal solid-state reaction and self-propagating high temperature reaction, respectively.

During the sliding process, $Cu_xNbSe_2/NbSe_2$ would be transferred to the friction surface to form the tribo-film. As $NbSe_2$ increased to 10wt.%, the tribo-film on the worn surface became complete and dense. Besides, TiB_2 with excellent mechanical properties existed uniformly on the tribo-film, which greatly resisted the plowing effect of counterpart to protect the Cu-based composites severe damage.

Acknowledgements

This research was financially supported by National Natural Science Foundation of China (51275213, 51302112), the Jiangsu National Nature Science Foundation (BK2011534, BK2011480), the Scientific and Technological Innovation Plan of Jiangsu Province in China (Grant Nos. CXLX13_645, CXZZ13_0669, KYLX_1029).

References

[1] X. Qiao, Q. Shen, L. Zhang, C. Lawson, X. Fan and H, Materials, Rare Metal. Mat. Eng. **43**, 2614 (2014).
[2]S. Biyik, F. Arslan and M. Aydin, J. Electron. Mater. **44**, 457**(** 2015).
[3] Z. Wang, Y. Zhong, X. Rao, C. Wang, J. Wang, Z. Zhang, W. Ren, Z. Ren, T. Nonferr. Metal. Soc. **22**,1106**(**2012).
[4] B. Ma, Q. Li, L. Li, G. Huang, L and Cheng, S. Xie, Rare Metal. Mat. Eng. **412**, 339**(**2012).
[5] P. Zhang, J. Jie, H. Li, T. Wang, T. Li, J. Mater. Sci. **50**, 3320**(**2015).
[6] Y.Watanabe, Wear. **264**, 624 **(**2008).
[7] S.G. Jia, P. Liu, F.Z. Ren, B.H. Tian, M.S. Zheng, G.S. Zhou, Wear. **262**,772 **(**2007).
[8] M.Grandin, U. Wiklund, Friction, Wear. **302**, 481 (2011).
[9] S.G. Jia, P. Liu, F.Z. Ren, B.H. Tian, M.S. Zheng , G.S. Zhou, Met. Mater. Int. **13**,25**(**2007).
[10] W. Wang, X. J. Liu , M. H. Jiao, Lubric. Eng. **11,**173**(**2007).
[11] S.C.Tjong , K.C.Lau, Materials Letters. **43**,274 **(**2000).
[12]A.K. Shukla, S.V.S.N. Murty, S.C. Sharma, K. Mondal, J. Alloy. Compd. **590**, 514 (2014).
[13] R.G. Zhang, X.M.Liu, Materials Research Innovations.**18**, 31(2014) .
[14] H. Tang, K. Cao, Q. Wu, C. Li, X. Yang, X. Yan, Cryst. Res. Technol. **46**,195 (2011) .
[15] J. M Harp, P. A. Lessing, R E Hoggan, Journal of Nuclear Materials. **466**,728 **(**2015).
[16] D. Wu, S. P. Wu, L .Yang, Powder Metallurgy. **58**,100 **(** 2015).
[17] T. Mimoto, J. Umeda, K. Kondoh, Powder Metallurgy. **59**, 223 **(**2016).
[18] Bei Bei Chen, Jin Yang, Qing Zhang, Hong Huang, HongPing Li, Hua Tang, ChangSheng Li, Material and Desgin. **75**, 24 **(**2015).
[19] H.Ashuri, A. Hassani, J. Alloy. Compd. **617**, 444 **(** 2014).
[20] J. M. Voorhoeve-Van Den Berg, Journal of the Less-Common Metals. **26**, 399 **(**1972).
[21] O. S. Rajora, A. E .Curzon, Physica Status Solidi (a). **97**, 65 (1986).
[22] Freund J, Wortmann G, Paulus W, Krone W, Journal of Alloys and Compounds. **187**, 1577 (1992).
[23] C.S. Ramesh, A. Ahamed, Wear. **271**, 1928 (2011).
[24] H.E.Sliney, ASLE Trans. **29**, 370 (1986).